Contract No.:

This manuscript has been authored by Battelle Savannah River Alliance (BSRA), LLC under Contract No. 89303321CEM000080 with the U.S. Department of Energy (DOE) Office of Environmental Management (EM).

Simulated Aging of Metal Tritides by Ball Milling Induced Gas Incorporation

by

Dustin Olson, Kirk Shanahan, Binod Rai, Dale Hitchcock, Catherine Housley, George Larsen*

Savannah River National Laboratory, Aiken, SC, 29808, USA

Abstract

The study of tritium aging effects on materials requires a significant time commitment as a consequence of its 12.3 year half-life, making developmental studies prohibitively difficult and expensive. However, detailed knowledge of long-term aging effects is critical to the development of structural and storage materials for future fusion reactor technologies. As a result, multiple approaches to simulated aging effects have been investigated. We report a method of simulated tritium aging achieved though the incorporation of trapped gases via high-energy ball milling of $LaNi_{4.25}Al_{0.75}$ alloy storage material. Experimental results verify the presence to trapped gases by a combination of temperature programmed desorption and LECO chemical analysis. Following gas incorporation, we find that many of the degraded hydrogen sorption properties found in aged storage materials are reproduced by the ball milled powders.

Keywords:
He Bubbles, Simulated Tritium Aging, Metal Tritides, Tritium

Highlights

- The incorporation of He/N_2 into $LaNi_{4.25}Al_{0.75}$ alloy by high-energy ball milling is confirmed by temperature programmed desorption (TPD) and LECO elemental analysis.
- Gas incorporation by ball milling reproduced many effects observed in the hydrogen sorption properties of a material due to tritium aging.
- Hydrogen cycling results in a redistribution of incorporated gas to lower-energy trap sites.

* Author to whom correspondence should be addressed

Email: george.larsen@srnl.doe.gov

1. Introduction

Metal hydride technologies for the storage and delivery of hydrogen isotopes are critical to meeting current and future tritium processing demands. This demand is expected to increase considerably with the increased global investment in D-T fusion reactor technology such as the International Thermonuclear Experimental Reactor (ITER) [1]. To date, the world's largest metal hydride-based tritium processing facility is located at the Savannah River Site (SRS) and is based primarily on $LaNi_{4.25}Al_{0.75}$ alloy, hereon referred to as LANA.75. LANA.75 beneficially retains nearly all the ^3He formed through decay during tritium storage. This feature facilitates the delivery of nearly pure tritium for gas mixture preparation. However, tritium aging changes the properties of LANA.75 over time due to ^3He retention [2], causing a significant reduction in storage capacity over an 8-10-year period and results in a quantity of trapped tritium known as a "heel," followed by the eventual release of ^3He. These changes in metal tritide properties can most notably be observed as dramatic changes to the pressure-composition-temperature (PcT) curve of a material. Properties such as equilibrium pressures that are a critical to the design and use in storage applications can be greatly affected [3].

In general, materials exposed to tritium accumulate ^3He as tritium diffuses into the material matrix and decays into ^3He by beta decay [4]. These ^3He atoms can then coalesce and form He nano bubbles that can grow to larger sizes and can cause deleterious effects on materials properties. For example, He bubble embrittlement of structural materials was studied at SRS as early as 1976 [5]. Investigations of He bubble formation, properties, and damage remediation are significantly limited by the methods currently available to generate them, which include tritium aging, He ion implantation, and neutron irradiation [6]. These techniques are costly, prohibitively time consuming, pose radiation hazards, create collateral ion damage, and are limited to the near surface

region in the case of implantation. Recently, it has been reported that mechanical alloying via ball milling can incorporate inert gases, such as Ar and He, into material matrices and subsequently produce numerous gas bubbles trapped in the metals [7-9].

This raises the possibility of preparing a simulated aged metal tritide by gas incorporation through ball milling for the investigation of effects on hydrogen sorption properties. The advantages of using ball milling to simulate aging are reduced costs and increased throughput compared to traditional tritium aging, in addition to removing the necessity for radiological safety considerations. This process will allow faster development of storage material regeneration processes, as well as enable investigations into new materials that may be more resistant to tritium aging effects, and ensuring safe, reliable, and predictable behavior of future materials. The following report investigates the effects of gas incorporation due to ball milling on the structural and hydride properties of LANA.75 and additionally confirms gas incorporation through a combination of LECO elemental analysis and temperature programmed desorption (TPD).

2. Material and Methods

2.1. Material Preparation

Preparation of gas-incorporated LANA.75 samples was performed by the addition of 30g of as received LANA.75 (Japan Metals and Chemicals, Co.,Ltd) to the grinding bowl of a high-energy, planetary ball mill (Fritsch Pulverisette) with stainless steel balls in a 10:1 ball to powder mass ratio. The mill was run at 500 rpm for 20 hours with a cycle duration of 30 min on and 30 min off. The container atmosphere of He or N_2 was established by evacuating the grinding bowl then backfilling to 10 psig with the respective gas. At the end of the milling run, an additional 10-

minute mill in ethanol was necessary to free the LANA.75 powder that had adhered to the side of the grinding bowl.

2.2. Analysis Methods

The desorption characteristics of He, H_2, D_2 from the powders were measured by TPD performed in an ultrahigh vacuum (UHV) system operating at a base pressure of 1 x 10^{-9} Torr. The system is pumped by means of turbo molecular pumps configured in series in order to reduce the natural hydrogen background. Thermal desorption spectra were collected using a Extrel MAX-50 quadrupole mass spectrometer (QMS) equipped with a sampling cone geometry ionizer placed in direct line of sight with the sample to reduce background gas detection. In addition, the empty sample holder was degassed at 730 °C prior to loading to ensure desorbed gases were generated primarily from the powder sample. Temperature profiles were programmed and controlled through a built in PID controlled by Leybold system software, allowing for temperature ramp control from (0.01-1.0 K/s) and a temperature range from 30 – 730 °C. In order to evaluate gas content in powder samples, a custom sample holder was designed based on the standard "Flag" style sample plate. The sample holder was designed with a small sample well for powder samples. In addition, it is designed to hold a ¼" VCR filter gasket affixed by four spring clasps in order to prevent contamination of the vacuum chamber with powder samples (Figure 1). The amount of powder used and QMS sensitivity was dependent on the desorption species of interest, for H_2 (~5mg sample, 950V multiplier, 10^7 gain), N_2 (~25mg sample, 1150V multiplier, 10^7 gain), and He (~25mg sample, 1150V multiplier, 10^9 gain).

Hydrogen sorption studies were carried out using a Sieverts' apparatus constructed primarily of ¼" stainless steel tubing connected by Swagelok VCR fittings. Hydrogen and Deuterium gas were supplied from gas cylinders of 99.999 % purity. Sample and manifold pressures were monitored

with MKS 10 000 Torr Baratron pressure transducers. The sample temperature was measured using a Type K thermocouple in direct contact with the sample with heating applied via insulated beaker heaters controlled by a PID.

Quantification of gas species (O,N,H) in the milled LANA.75 samples was performed by means of LECO elemental analysis (LECO 836). Briefly, samples are weighed and placed into the combustion chamber where the sample is melted (1500 °C), resulting in the release of any trapped gas species. The released gases are subsequently quantified through the use of infrared (IR) and thermal conductivity (TC) detectors.

Milled LANA.75 powder was characterized using a particle size analyzer (Bettersizer S3 +) utilizing laser diffraction. Scanning electron microscopy was conducted using a Hitachi SU8200 series cold field emission (CFE) SEM. The crystal structure of the powders milled under the various atmosphere, and before and after heating to 730 °C was analyzed with an X-ray Diffractometer (XRD, Panalytical X'Pert Pro 3040). Rietveld refinement or Le Bail fitting (FullProf) was performed to determine the crystal phases present in the materials.

3. Results and Discussion

3.1. Microstructural Analysis

Microstructural analysis was performed by XRD to compare the crystalline properties and material phases present in the LANA.75 powders prepared under He or N_2 milling atmospheres, in addition to the pristine powder. Figure 2 displays the measured XRD pattern for the milled samples under He or N_2 compared to the pristine LANA.75. It can be seen that the peak intensities decrease concomitantly with a broadening of the diffraction peaks for the milled materials, which indicates

a decrease in the crystalline quality induced by the milling process. However, the peaks present are all consistent with those expected in the pristine materials.

The crystalline properties of the materials were investigated following gas desorption at 730 °C , to determine the changes, if any, present in the powders (Fig. 2). After heating to 730 °C under vacuum, the He milled sample (Fig. 2a) shows the presence of additional phases corresponding to Ni_3Al, while heating of pristine LANA.75 (Fig. 2c) displays no measurable differences. Additionally, the N_2 milled sample (Fig. 2b) following heating to 730 °C shows the growth of additional phases Ni_3Al and La_2O_3. These results are consistent with the findings for the regeneration of tritium aged LANA.75 beds heated to (1000 °C), which also resulted in the emergence of the Ni_3Al phase [10].

Table 1 summarizes the particle sizes measured by laser diffraction for the various LANA.75 powders investigated in this study. Ball milling of the pristine material results on average in an approx. 96% (D90) reduction in particle size compared to the pristine powder. In addition, following hydrogen cycling there is a further reduction in particle size of approx. 7% (D90), resulting from the expected material decrepitation during the hydrogen absorption-desorption.

Particle morphology was investigated using scanning electron microscopy (SEM), and representative SEM images of He milled are presented in Figure 3. The particle morphologies are consistent with previous descriptions of lanthanum nickel-based alloys, having flat, fractured surfaces and irregular shapes. No notable changes are observed in the milled particles after hydrogen cycling and/or heating to 730 °C.

3.2. Hydrogen Sorption Behavior

The hydrogen sorption properties of the various LANA.75 samples were characterized by a Sievert's apparatus as describe above. Figure 3a presents the 80 °C desorption isotherms for pristine, He milled, and N_2 milled LANA.75 samples. The milled samples display a greatly reduced hydrogen capacity decreasing from pristine (0.73 H/M) > He Milled (0.53 H/M) > N2 milled (0.37 H/M), a sloping and narrower plateau region, and the presence of a heel indicating trapped hydrogen. Figure 3b displays a series of isotherms collected for a He milled powder sample at 53 °C, 80 °C, and 120 °C. The average plateau pressures are used to calculate the thermodynamic properties of the He milled sample for comparison to the pristine material (Inset: Figure 3b) showing a negligible change in both enthalpy and entropy.

The degradation in hydride performance of the milled samples is comparable to the observation for tritium aged samples [11], with the exception that in the case of the milled samples the equilibrium plateau pressures, and hence, thermodynamic properties appear unchanged. These differences can likely be attributed to the location the trapped gases reside within the LANA.75 matrix. In the case of the milled samples the trapped gas is likely to reside in defects, grain boundaries, and between surfaces. While in the case of true tritium aged samples, the He born in the lattice occupies interstitial sites until such time that the clusters reach a critical size and diffusion to grain boundaries can occur [12]. These observations together suggest the following role of trapped helium: at first interstitially trapped species cause lattice strain resulting in a decrease in plateau pressures, while helium agglomerated in grain boundaries and defects results in further detrimental effects such as reduced capacity, and a trapped heel (Fig. 3A).

3.3. LECO Chemical Analysis

In order to measure quantitative amounts for the incorporated gases, LECO elemental analysis was performed allowing the amounts of hydrogen, oxygen and nitrogen present in the milled and pristine LANA.75 samples to be measured. Table 2 shows the O, N, H contents measured for the various samples reported as ppm quantities. As seen in Table 2 there is a significant increase in the oxygen content for the milled samples. This scales with surface area as both milling and hydrogen cycling reduces the particle size (Table 1), thereby increasing the surface area available to oxidation. The propensity of lanthanum nickel alloys to rapidly form oxides is well established and is due to a segregation and disproportionation to La oxide and metallic Ni [13], resulting from a large heat of formation of La_2O_3. In addition, we observe a significant increase in the nitrogen concentration due to ball milling under a nitrogen atmosphere. The amount of nitrogen incorporated can be used to approximate an equivalent loading of ^3He in tritium aged material. Assuming a 1:1 correspondence with ^3He and full loading of 0.6 H/M, the nitrogen incorporated during milling is equivalent of ~3.8 years of aging. In general, there is an increase in hydrogen content for milled samples, which may be related to surface hydroxides or to the ethanol milling process during release. Finally, there is a large increase in hydrogen content for the hydrogen cycled sample, which indicates that the damage due to gas incorporation and milling results in hydrogen trapping, consistent with the heel observed in PcT curves for the milled samples.

These results demonstrate that gas, in the above case, nitrogen, can be incorporated into the LANA.75 lattice via ball milling to concentration levels that correspond to nearly 4 years of aging. Park et al. [9], have previously demonstrated that the levels of gas incorporation during milling is energy dependent. This suggests that simulated material ages could be achieved though optimization of the milling process parameters, such as energy, gas pressure, and milling temperature. There is also the potential that ball milling under nitrogen has the potential to produce

chemistry induced mechanochemically [14]. However, the lack of new phases present in XRD data for milled samples suggests the nitrogen is incorporated primarily in the gaseous state.

3.4. Temperature Programmed Desorption (TPD)

To investigate the desorption characteristics of gases (He, N_2, H_2) from the powder samples we employed TPD, a technique widely applied to the study of He desorption in materials [15, 16]. Figure 5 shows the resulting TPD profiles for H_2 desorption from the He and N_2 milled LANA.75 before and after hydrogen cycling. For the He milled sample a single broad desorption peak centered at 425 °C is observed. With hydrogen cycling, there is a growth in peak area consistent with the observation of trapped hydrogen in the PcT curves. In addition, this peak shifts to a lower temperature centered at 400 °C, which is consistent with a second order desorption process expected for recombinative desorption. The desorption of H_2 from the N_2 milled sample occurs over a similar temperature range, however, the N_2 milled sample features a shoulder at higher temperature centered at 510 °C indicating hydrogen trapped in an additional site. With hydrogen cycling, we again observe a growth in peak area, however, in this case it is not accompanied by a clear shift in peak temperature.

Figure 6a, shows the resulting desorption profiles for He from the milled LANA.75 powders. Assuming the desorption of helium is governed by first-order kinetics, the desorption activation energy E_{des} can be calculated according to the following equation [17],

$$E_{des} \approx RT_p \left[ln\left(\frac{\nu_1 T_p}{\beta}\right) - 3.64 \right] \quad (1)$$

Where E_{des} is the desorption activation energy per mole He, ν is the so-called frequency factor describing the rate at which jumping events occur, which is generally approximated as 10^{13}/s, R is the gas constant, T_p is the peak temperature corresponding to maximum desorption rate for a

particular process, and β is the heating rate in K/s. Equation (1) provides a method of estimating the desorption energy associated with the peaks observed for helium desorption from the milled LANA.75 powders. Applying the above approximation to the obtained He desorption profiles (Figure 6a) we obtain the following desorption energies P_1 (2.166 eV), P_2 (2.415 eV), P_3 (2.695 eV) for the respective peaks. We can apply the same approximation to the multiple observed peaks in the N_2 desorption profile (Figure 6b), in which case we obtain desorption energies of L_1 (2.05 eV), L_2 (2.15 eV), and L_3 (2.55 eV), assuming again a first order desorption process. In the case of N_2 desorption it is clear from the TPD profile that all of the trapped gas has not desorbed by 730 °C, evidenced by the rising profile intensity at the end of the measurement. The similarity between desorption energies, particularly in the case of (P_1:L_2) suggest the occupation of identical trap sites in the material matrix between the two samples.

Reliable detection of He desorption from the LANA.75 samples required an increase in QMS preamplifier gain from 10^7 used for H_2/N_2 to a gain of 10^9 for He during TPD experiments. At a constant multiplier voltage this indicates a much greater incorporation of N_2 over He gas during the milling process. This observation is in accord with the intensified detrimental effects observed in both the hydrogen sorption and crystalline properties of the nitrogen milled sample. This is in great agreement with previous experiments that showed milling in N_2 atmosphere resulted in the greatest incorporation of gas species into an iron-based alloy [8].

The observation of multiple desorption peaks for He has been previously observed in Fe base alloys [15, 18], and are attributed to different trap sites at increasing energies such as interstitial helium, vacancy-clusters, and helium bubbles, respectively. Due to the temperature limit of our instrument (730 °C) it is likely that there are higher energy trap sites that lay outside of our detectable window, as He desorption at temperatures greater than 927 °C are common [18]. In

Figure 5a,b we see an increased QMS signal for both the He/N_2 milled-H_2-cycled samples suggesting a greater content of incorporated gases. However, the cycled samples originated from the same milling vessel as the uncycled material and no He/N_2 was present in the atmosphere during cycling, and further, the LECO analysis above shows that the total nitrogen content is the equivalent in the N_2 milled samples before and after hydrogen cycling. Thus, another explanation is necessary. As mentioned above it is very possible that higher energy trap sites exist in these materials, and it is likely that strains in the material matrix caused by hydriding cause a redistribution of the trapped gas species to lower energy sites likely more near the surface. A similar phenomena was previously observed with the cycling of tritium aged materials that resulted in a moderate recovery of hydride performance [11].

In order to develop a more detailed understanding of the specific trap sites occupied by the entrained gases we can compare the desorption energies to the results of positron annihilation lifetime (PAL) experiments performed on a similar hydrogen storage material $LaNi_5$ [19, 20]. In the temperature range below 430 °C a large migration of small vacancies and vacancy clusters was observed by PAL. The similarity in measured desorption temperature suggests this is the primary location of trapped H_2 in our materials. In addition, it was shown that removal of particular dislocations in $LaNi_5$ occurs between 550 °C – 700 °C while others remain to temperatures greater than 950 °C, indication that incorporated He and N_2 reside largely in dislocations. Lastly, Shirai et al [20], also demonstrated that hydrogen absorption results in a significant formation of vacancies and vacancy clusters. This is likely the associated mechanism resulting in the redistribution of He, N_2 in the material observed after hydrogen cycling.

4. Conclusion

The hydrogen sorption properties of LANA.75 powders following gas incorporation facilitated by ball milling were studied by PcT. It is observed that the ball milling process reproduced many important features observed as a result of tritium aging, such as reduced capacity and a trapped heel. The relative effect of gases trapped interstitially compared to those at grain boundaries is proposed based on the likely location of trapped gases resulting from the ball milling process. The precise location and composition of non-lattice gases needs further investigation through additional techniques, such as transmission electron microscopy (TEM) and electron energy loss spectroscopy (EELS). However, gas incorporation was confirmed by a combination of TPD, and LECO elemental analysis performed on the powders for the detection of He and N_2. The observed changes to the hydrogen sorption properties with ball milling demonstrate the potential for the preparation of simulated tritium aged materials, thus providing an avenue toward the rationalization of tritium aging experiments.

Acknowledgements

The authors wish to acknowledge Prabhu Ganesan for technical support on the project and would also like to thank Jim Klein, Harry García Flores, and Greg Staack for helpful discussions and direction. The authors gratefully acknowledge the NNSA Office of Tritium Modernization for funding this work. This work was produced by Battelle Savannah River Alliance, LLC under Contract No. 89303321CEM000080 with the U.S. Department of Energy. Publisher acknowledges the U.S. Government license to provide public access under the DOE Public Access Plan (http://energy.gov/downloads/doe-public-access-plan). The United States Government retains and the publisher, by accepting this article for publication, acknowledges that the United States

Figure Captions

Figure 1. Custom powder sample holder, (a) Front view with gasket above surface. (b) Cross-section showing sample pocket when gasket is in place.

Figure 2. XRD data for pristine and milled samples compared to each sample following heating to 730 °C under vacuum, (a) N_2 milled, (b) He milled, and (c) pristine LANA.75. Where (*) indicates impurity phases consisting of La_2O_3 and Ni_3Al.

Figure 3. Representative scanning electron microscopy images of He milled samples (a) after milling, (b) after heating to 730 °C, (c) after H_2 cycling, and (d) after H_2 cycling and heating to 730 °C. Scale bars are 5μm.

Figure 4. (a) 80 °C desorption isotherms for pristine, He milled, and N_2 milled LANA.75 samples. (b) PcT curves for He milled LANA.75 at three indicated temperatures. Inset: thermodynamic properties obtained from Van't Hoff plot compared to properties of pristine material.

Figure 5. H_2 (2 amu) TPD for He/N_2 milled and milled-cycled samples. Each plot is normalized to the sample mass used (~5.0 mg).

Figure 6. (a) He TPD (4amu) milled and H_2 cycled, (b) N_2 TPD (28amu) milled and H_2 cycled. Each plot is normalized to the sample mass used (~25.0 mg).

Paper Figures

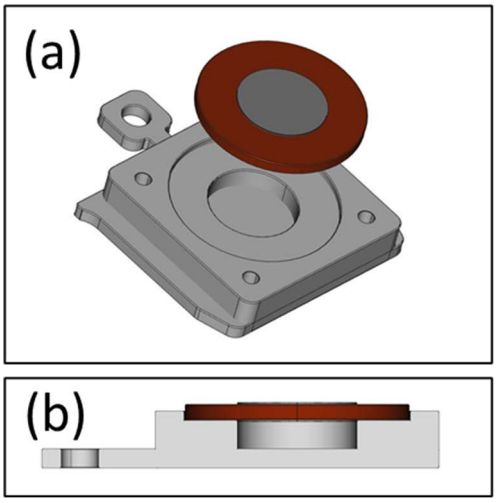

FIGURE 1.

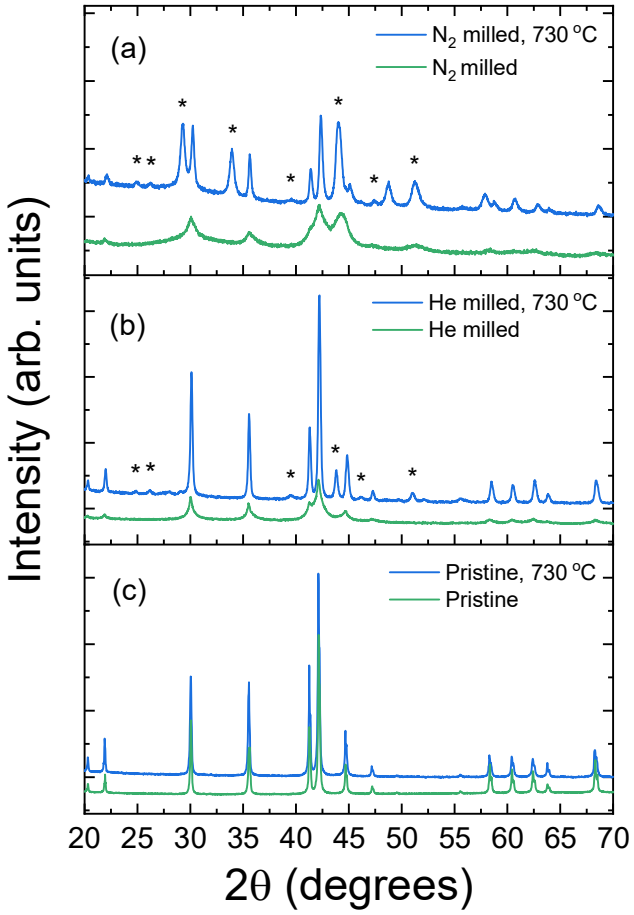
(a)
N2 milled, 730 °C
N2 milled
(b)
He milled, 730 °C
He milled
(c)
Pristine, 730 °C
Pristine
Intensity (arb. units)
20 25 30 35 40 45 50 55 60 65 70
2θ (degrees)

FIGURE 2.

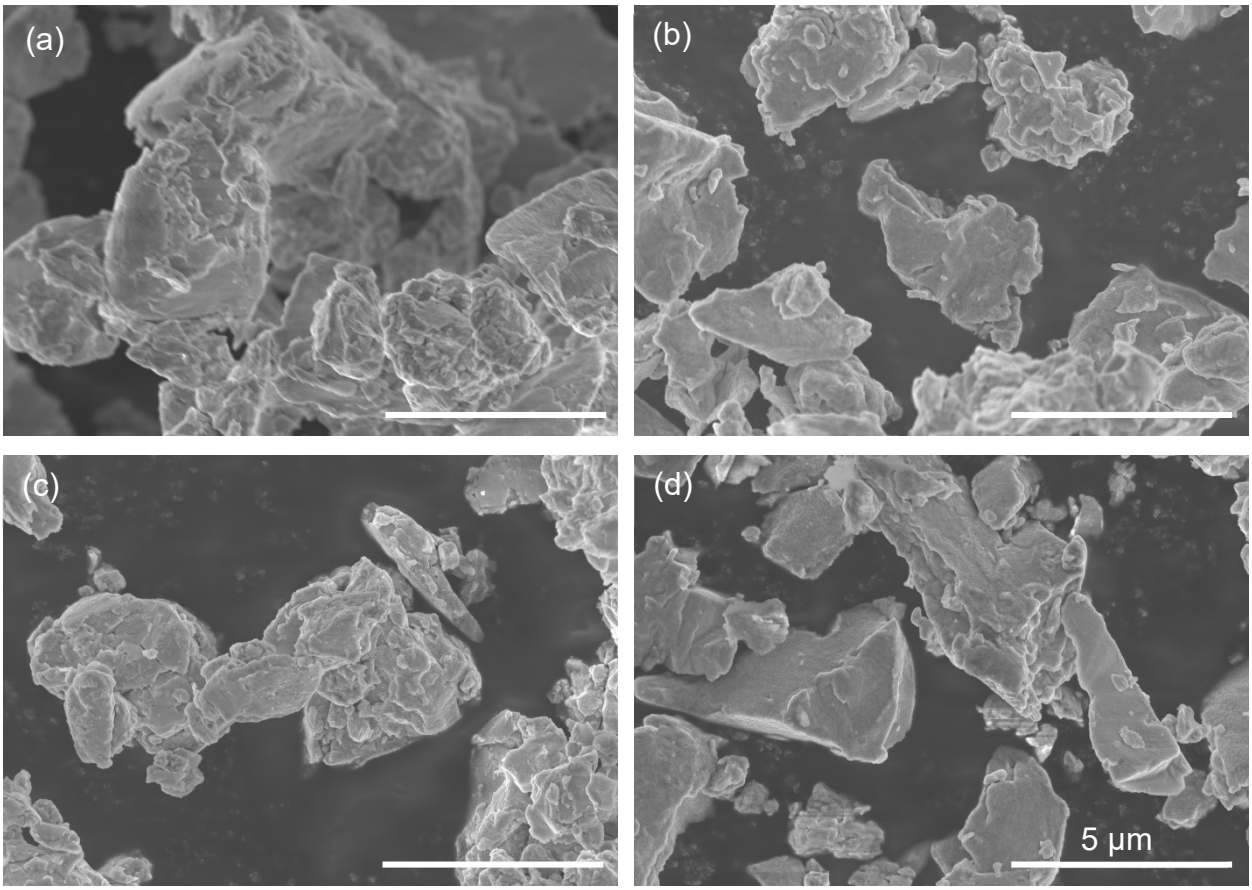

FIGURE 3.

LANA.75 Sample	Particle Size (μm) D10	D50	D90
Pristine	7.99	80.85	311.70
He milled	2.40	5.09	9.80
He milled, H_2 cycled	1.87	4.26	9.02
N_2 milled	2.68	6.06	13.02
N_2 milled, H_2 cycled	2.66	5.73	12.20

TABLE 1

LANA.75 Sample	Oxygen (ppm)	Nitrogen (ppm)	Hydrogen (ppm)
Pristine	1190 ± 80	101 ± 8	42 ± 4
He milled	12300 ± 200	283 ± 9	400 ± 2
N_2 milled	12700 ± 300	26500 ± 800	334 ± 9
N_2 milled, H_2 cycled	14900 ± 600	25000 ± 1000	1130 ± 60

TABLE 2.

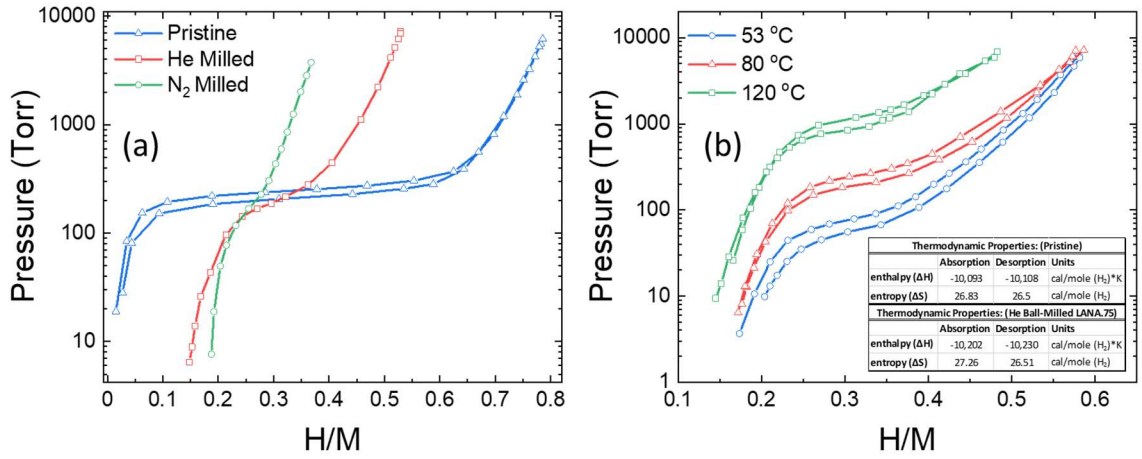
Pristine
He Milled
N2 Milled
(a)
Pressure (Torr)
H/M
53 °C
80 °C
120 °C
(b)
Pressure (Torr)
H/M
Thermodynamic Properties: (Pristine)
Absorption Desorption Units
enthalpy (ΔH) -10,093 -10,108 cal/mole (H2)*K
entropy (ΔS) 26.83 26.5 cal/mole (H2)
Thermodynamic Properties: (He Ball-Milled LANA.75)
Absorption Desorption Units
enthalpy (ΔH) -10,202 -10,230 cal/mole (H2)*K
entropy (ΔS) 27.26 26.51 cal/mole (H2)

FIGURE 4.

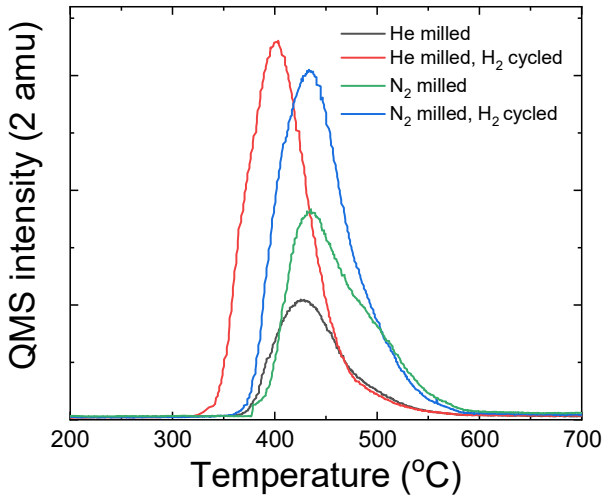
He milled
He milled, H2 cycled
N2 milled
N2 milled, H2 cycled
QMS intensity (2 amu)
200
300
400
500
600
700
Temperature (°C)

FIGURE 5.

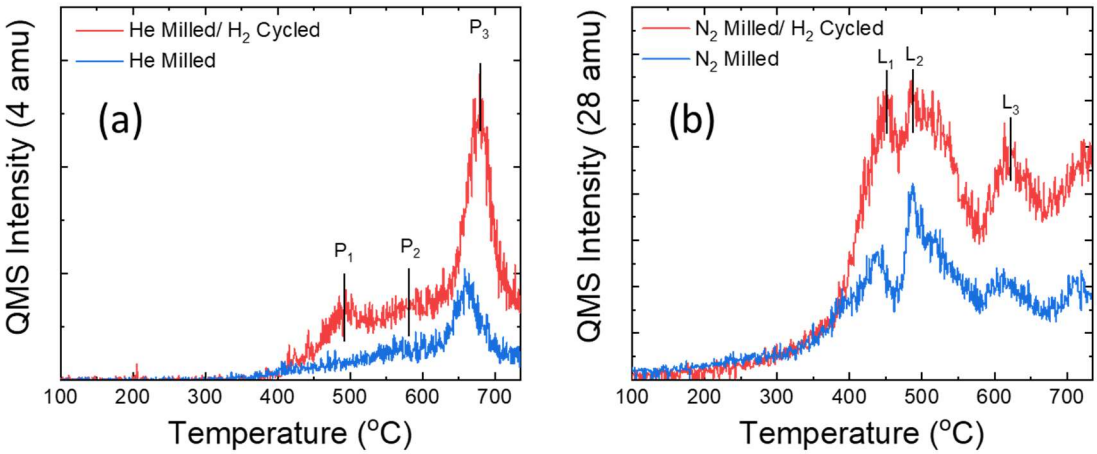
He Milled/ H2 Cycled
He Milled
(a)
P1
P2
P3
QMS Intensity (4 amu)
Temperature (°C)
N2 Milled/ H2 Cycled
N2 Milled
(b)
L1
L2
L3
QMS Intensity (28 amu)
Temperature (°C)

FIGURE 6.

References

1. Pearson, R.J., A.B. Antoniazzi, and W.J. Nuttall, *Tritium supply and use: a key issue for the development of nuclear fusion energy.* Fusion Engineering and Design, 2018. **136**: p. 1140-1148.
2. Shanahan, K.L., et al., *Tritium aging effects in LaNi4.25Al0.75.* Journal of Alloys and Compounds, 2003. **356-357**: p. 382-385.
3. Thiébaut, S., et al., *3He retention in LaNi5 and Pd tritides: Dependence on stoichiometry, 3He distribution and aging effects.* Journal of alloys and compounds, 2007. **446**: p. 660-669.
4. Lässer, R., *Tritium and helium-3 in metals*. Vol. 9. 2013: Springer Science & Business Media.
5. Donovan, J., *Effects of helium on mechanical properties of Armco iron*. 1976, Du Pont de Nemours (EI) and Co., Aiken, SC (USA). Savannah River Lab.
6. Rabaglino, E., *Helium and tritium in neutron-irradiated beryllium*. Vol. 6939. 2004: FZKA.
7. VanLeeuwen, B.K., et al., *Novel technique for the synthesis of ultra-fine porosity metal foam via the inclusion of condensed argon through cryogenic mechanical alloying.* Materials Science and Engineering: A, 2011. **528**(4): p. 2192-2195.
8. Muramatsu, Y., et al., *Gas contamination due to milling atmospheres of mechanical alloying and its effect on impact strength.* Materials transactions, 2005. **46**(3): p. 681-686.
9. Park, E.-K., et al., *Reduced argon bubble formation in oxide dispersion strengthened steels by high-energy mechanical alloying.* Scripta Materialia, 2016. **113**: p. 31-34.
10. Staack, G., M. Crowder, and M. Tosten, *Controlled Oxidation of Tritium-Aged LaNi4. 25Al0. 75 Hydride to Support Retired Bed Disposition.* SRNL-STI-2015-00004, 2015.
11. Nobile, A., J. Wermer, and R. Walters, *Aging effects in palladium and LaNi4. 25Al0. 75 tritides.* Fusion Technology, 1992. **21**(2P2): p. 769-774.
12. Cowgill, D.F., *Helium nano-bubble evolution in aging metal tritides.* Fusion science and technology, 2005. **48**(1): p. 539-544.
13. Schlapbach, L. and C. Brundle, *XPS study of the chemisorption induced surface segregation in LaNi5 and ThNi5.* Journal de Physique, 1981. **42**(7): p. 1025-1028.
14. Senna, M. and K. Okamoto, *Rapid synthesis of Ti-and Zr-nitrides under tribochemical condition.* Solid State Ionics, 1989. **32**: p. 453-460.
15. Wang, L., et al., *Helium desorption behavior and growth mechanism of helium bubbles in FeCrNi film.* Nuclear Materials and Energy, 2019. **21**: p. 100710.
16. Cheng, G., et al., *Thermal desorption behavior of helium in aged titanium tritide films.* Journal of Nuclear Materials, 2015. **466**: p. 615-620.
17. Redhead, P., *Thermal desorption of gases.* vacuum, 1962. **12**(4): p. 203-211.
18. Ono, K., et al., *Release of helium from irradiation damage in Fe–9Cr ferritic alloy.* Journal of nuclear materials, 2004. **329**: p. 933-937.
19. Sakaki, K., H. Araki, and Y. Shirai, *Recovery of hydrogen induced defects and thermal desorption of residual hydrogen in LaNi5.* Materials transactions, 2002. **43**(7): p. 1494-1497.
20. Shirai, Y., H. Araki, and K. Sakaki, *Positron annihilation study of hydrogen storage alloys*. 2003.